Multispectral image analysis of bruise age

Stephen Sprigle[*a], Dingrong Yi[b], Jayme Caspall[a], Maureen Linden[a], Linghua Kong[a], Mark Duckworth[a]

[a]Center for Assistive Technology and Environmental Access, College of Architecture, Georgia Institute of Technology, 490 Tenth Street, NW, Atlanta, Georgia 30332-0156, U.S.A.

[b]Imaging Research, Sunnybrook Health Sciences Centre & Medical Biophysics Department of University of Toronto, Room S-646, 2075 Bayview Avenue Toronto, ON M4N 3M5, Canada

ABSTRACT

The detection and aging of bruises is important within clinical and forensic environments. Traditionally, visual and photographic assessment of bruise color is used to determine age, but this substantially subjective technique has been shown to be inaccurate and unreliable. The purpose of this study was to develop a technique to spectrally-age bruises using a reflective multi-spectral imaging system that minimizes the filtering and hardware requirements while achieving acceptable accuracy. This approach will then be incorporated into a handheld, point-of-care technology that is clinically-viable and affordable. Sixteen bruises from elder residents of a long term care facility were imaged over time. A multi-spectral system collected images through eleven narrow band (~10 nm FWHM) filters having center wavelengths ranging between 370-970 nm corresponding to specific skin and blood chromophores. Normalized bruise reflectance (NBR)- defined as the ratio of optical reflectance coefficient of bruised skin over that of normal skin- was calculated for all bruises at all wavelengths. The smallest mean NBR, regardless of bruise age, was found at wavelength between 555 & 577nm suggesting that contrast in bruises are from the hemoglobin, and that they linger for a long duration. A contrast metric, based on the NBR at 460nm and 650nm, was found to be sensitive to age and requires further investigation. Overall, the study identified four key wavelengths that have promise to characterize bruise age. However, the high variability across the bruises imaged in this study complicates the development of a handheld detection system until additional data is available.

Keywords: feature extraction, optical imaging, detection, bruise, bruise age, bruise color, multi-spectral imaging, tissue reflectance, skin reflectance, image cube

1. INTRODUCTION

Elder and child abuse is becoming a problem of our modern society. A 2003 national report estimated that 1 to 2 million elder Americans (age 65 or older) have been injured, exploited or otherwise mistreated by someone on whom they depended for care or protection[1]. The 1998 NCEA Incidence study found that in 1996, nearly 450,000 elders (≥ age 60) were abused and/or neglected in home settings; of those, 30% were physically abused[2].

The most current statistics from the U.S. Department of Health and Human Services, Administration on Children, Youth and Families reflect that for the year 2003, more than 4 (4.11) children die per day as a result of child abuse in the home[3]. The actual child abuse/neglect incidence rate is estimated at three times greater than the number of reported cases[4]. Quantitative characterizing and age determining is an effective way for the assessment and prevention of abuse. However, analysis of bruises, particularly aging of bruises based on visual appearance alone (color), either in vivo or via photographs, has not been deemed reliable, especially in children[5,6,7,8]. It should be noted, that among the bruise aging studies, dark-skinned subjects are not well represented. An increased concentration of melanin complicates bruise imaging by decreasing the contrast between bruised skin and normal skin. The requirement to assess individuals of all skin types further emphasizes the need of an improved means to determine the age of a bruise, beyond the capabilities of the naked eye.

During investigations of potential child and elder abuse, clinicians and forensic practitioners are often asked to offer opinions about the age of a bruise. Visual inspection in vivo and photography of bruises are two conventional methods employed in clinical practice. These methods, however, are qualitative, subjective, and inaccurate. Statistics indicate that their best accuracy is only about 50%[8,9,10,11]. Further, their failure rate is even much higher if bruises happened on darkly pigmented skin.

Recently spectroscopy has emerged to improve the reliability of bruise detection. The method allows one to infer the fractional contents of various chromophores (oxy-hemoglobin (oxyHb), deoxy-hemoglobin (deoxyHb), bilirubin,

Medical Imaging 2007: Computer-Aided Diagnosis, edited by Maryellen L. Giger, Nico Karssemeijer,
Proc. of SPIE Vol. 6514, 65142T, (2007) · 1605-7422/07/$18 · doi: 10.1117/12.709930

melanin) by measuring the optical reflectivity of one sample point at a time of bruised region for a continuous range of wavelength at fine steps (e.g., at 2nm incremental step). It is a reliable tool to investigate the basic biochemical processes associated with bruised skin on both white and darkly pigmented skin. However, point spectroscopy is too time consuming and tedious to create a distribution map of the chromophores concentration over time. Such a map is important since it contains the extrinsic features of the discoloration such as its shape and size, from which age is often inferred[12].

Full function spectrometers and multi-spectral imaging systems have demonstrated objectivity in identifying age-dependent features[13,14]. These devices are not well suited for clinical environments due to the complexity of implementation. The purpose of this study was to develop a technique using a fixed, discrete set of important wavelengths that reflect the age of bruises. This approach will then be incorporated into a handheld, point-of-care technology that targets bruises and is clinically-viable and affordable.

2. METHODS

Images were acquired of bruises incurred in normal activity from thirteen residents of an extended care facility. Table 1 lists the age, gender, ethnicity, location, and the approximate ages of bruises when imaged. Figure 1 identifies the locations of the bruises for each subject.

Bruise ID	Age	Race	Sex	Bruise Location	Num. Image Sets	Reported Age of Bruise at Measurement (days)
A	86	cauc.	M	Left forearm	2	14, 27
B	86	cauc.	M	Right forearm	2	14, 27
C	85	cauc.	F	Left lower leg	4	14, 20, 24, 27
D	86	cauc.	M	Left forearm	4	2, 6, 9, 13
E	72	cauc.	F	Right forearm	9	6, 10, 13, 17, 20, 27, 31, 40, 43
F	76	afr.	F	Top of left hand	4	8, 11, 15, 18
G	76	afr.	F	Top of right hand	4	9, 12, 23, 30
H	85	cauc.	F	Left lower leg	7	13, 20, 24, 27, 31, 40, 47
I	86	cauc.	M	Left forearm	1	3, 6
J	74	cauc.	F	Right thigh	1	7, 10
K	85	cauc.	F	Top of left hand	2	24, 28
L	82	cauc.	F	Left arm @ elbow	1	24, 28
M	82	cauc.	F	Right arm	1	5, 9
N	39	cauc.	M	Right Upper leg	7	1, 2, 5, 6, 12, 13, 14
O	80	cauc.	F	Right forearm	1	29
P	82	cauc.	F	Right front arm	3	8, 11, 15

Table 1: Information on bruises and subjects included in the study.

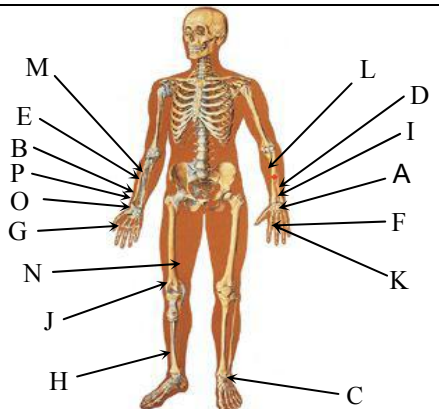

Figure 1. Anatomical location of bruises.

2.1 Imaging System

The multispectral image acquisition system consisted of a monochrome CCD camera mounted behind a twelve-position motorized filter wheel (Figure 2). The camera was a fire-i^{TM} board monochrome CCD camera from Unibrain Inc.

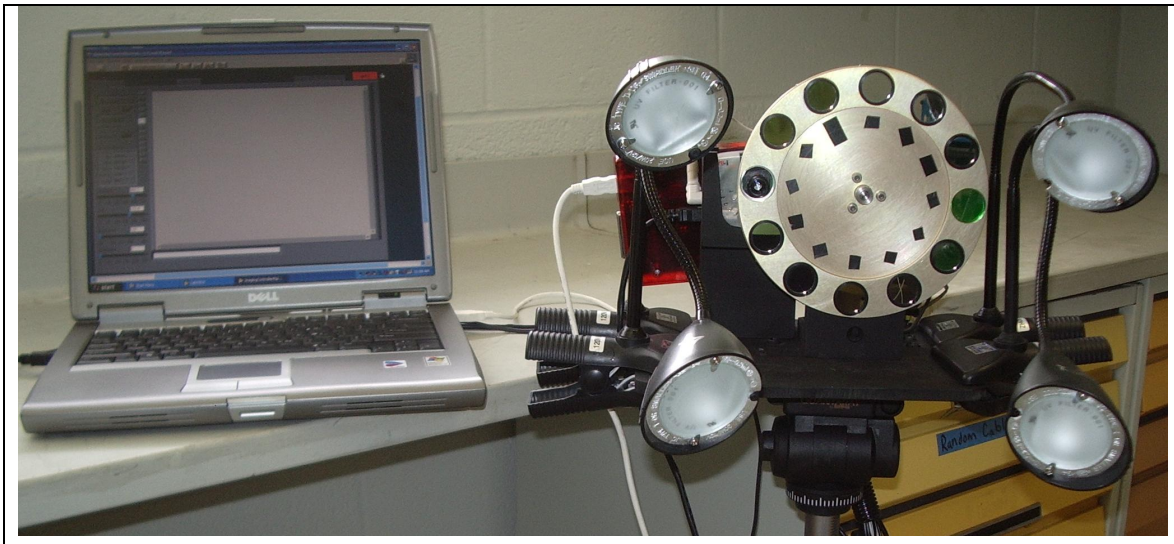

Figure 2. Imaging system.

The twelve-position filter wheel was populated with eleven narrow band (~10nm width) optical filters (370nm, 415nm, 460nm, 480nm, 540nm, 555nm, 560nm, 577nm, 650nm, 800nm, 970nm), leaving the twelfth position open. The filters were selected to target the absorption peaks of the primary chromophores of blood and skin, as shown in Figure 3. In particular, filters were chosen with center wavelengths on the bilirubin peak at 460 nm, the oxygenated hemoglobin peak at 540 nm, the local oxygenated hemoglobin trough at 560 nm (also very near the deoxygenated hemoglobin peak at 555 nm), and the oxygenated hemoglobin peak at 577 nm. The illumination is provided by four 35-watt, 12V AC, halogen lamps, each of which generates broadband illumination approximately equivalent to a 3200 K blackbody radiator, peaking near 900 nm. The four halogen lamps were mounted on "gooseneck" supports, allowing for flexible light placement to accommodate various body positions.

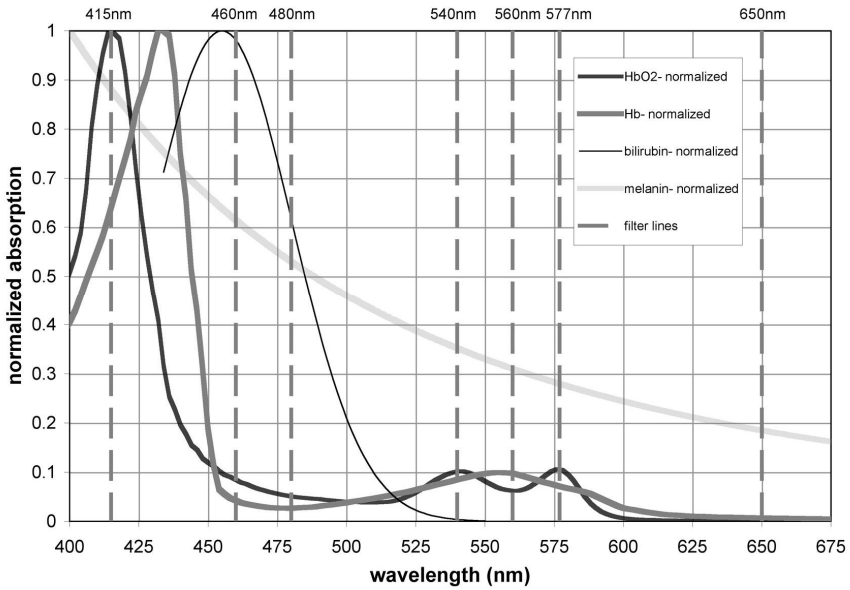

Figure 3. Normalized absorption curves with filter center wavelengths indicated as vertical dashed lines. From left to right the filter center wavelengths represented in the graph are 415 nm, 460 nm, 480 nm, 540 nm, 560 nm, 577 nm, and 650 nm.

2.2 Imaging procedure

General information about the subject such as age, gender, onset date of the bruises, skin-color were recorded (Table 1). For the first visit, the bruised area was visually identified and a purple surgical marker ink pen was used to enclose the selected bruised area in order to identify the bruise for future measurements. The subject was placed in a comfortable position such that the interest area is within 50cm away and roughly perpendicular to the camera viewing direction. The subject was instructed to remain still during the acquisition. Upon triggering the system, the rotating filter wheel sequentially brought the filters in front of the camera lens. Eleven filtered images and one unfiltered image were acquired and saved to disk in a single image "cube" file for each bruise sample session. For many subjects, the targeted area of the skin surface was covered by a matte sheet, and a reference "cube" was acquired with the subject position, camera position and viewing direction remained unchanged. This latter set was used in a shading correction procedure. Most of the data acquired in our study were bruise images without paper references. We adopted a quadric surface fit correction procedure to help reduce error in these images. In the results presented here, we used the fitting procedure for curvature correction and used validated it by comparison to the paper reference corrections.

2.3 Preprocessing

Preprocessing included four sequential steps. First, the image was rotated to align the principal axis of the bruise area to the rectangular coordinates of the image display. This step allowed for our rectangular ROI selection tools to more-or-less conform to the boundaries of the problem. Secondly, the image was cropped to include only skin in the vicinity of the bruise, while avoiding discontinuities unrelated to the local skin around the bruise, such as objects in the background beyond the skin horizon. In the cropping step, we endeavored to include enough normal skin to allow for curvature correction. Since the bruised skin darkens the image locally, the pixels corresponding to the bruise must be eliminated from the image prior to implementing the quadric fit curvature correction algorithm. Because of the large variation in bruise sizes and locations relative to the skin horizon, it was not always possible to provide cropped images with a field of normal skin surrounding the bruised skin. After cropping the image, the third preprocessing step was selecting ROIs for bruised skin and normal skin. One rectangle was used within the bruise boundary to select bruised skin pixels, and four rectangles were taken outside the bruise, providing four samples of normal skin at various locations near the bruise. The fourth and final step in the process involved selecting a circumscribed rectangle about the bruise to indicate the region of the image to be removed before determining the best quadric shading fit to the image for curvature correction. This four-step procedure was carried out for each image cube to be analyzed.

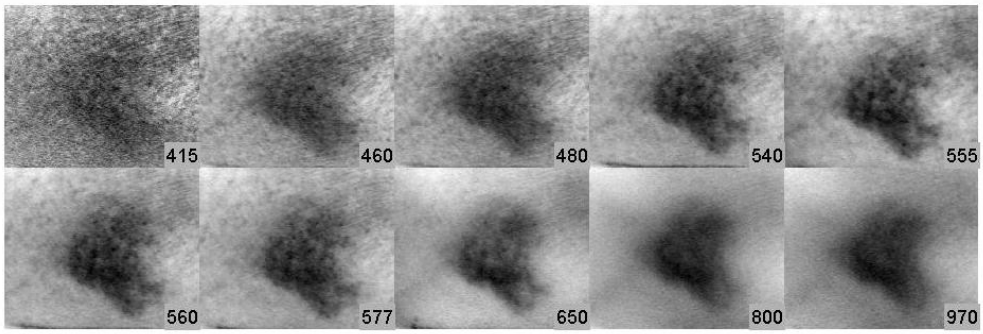

Figure 4. Typical multispectral images obtained with different optical filters in front of the CCD camera. The images have been scaled to provide a uniform range of values through each filter. The center wavelength for the image is indicated in the lower right hand corner of each image. This bruise was two weeks old in these images and resolved very slowly. The excellent contrast of the long wavelengths indicates that this is a deep bruise.

2.4 Analysis

Visual inspection of the multi-spectral images indicated that the bruise area appears darker and has lower pixel intensity than the normal skin surface (Figure 4). Contrast is the primary information and depends on the absorption peaks of chromophores that are commonly found in bruises (Figure.3). Conventionally light reflectance coefficient is defined as the ratio of light intensity reflected off the skin over that incidence.

$$\mu_{bruise} = \frac{I_{light\_intensity\_reflected\_from\_bruise}}{I_{Incident\_light\_on\_bruise}} \quad (1)$$

$$\mu_{normal} = \frac{I_{light\_intensity\_reflected\_from\_normal\_skin}}{I_{incident\_light\_on\_nromal\_skin}} \tag{2}$$

Assume (i) incident light are parallel rays and have homogenous distribution over the interested area of skin surface (ii) the light ray reflected off the surface skin are parallel and are focused by the camera lens and received by the CCD array which in turn presumably linearly convert them into electrical charges first then voltage signals. The magnitude of the voltage signals are sampled, digitized and stored as digital image. It is conventionally assumed that the all signal transformation procedures involved within the CCD camera are linear. If we further assume that all of the light energy received by the CCD camera were coming from the interested area of surface skin, i.e., there is no white noises resulted from the background lights or light that scattered from other object to cause CCD charges. Then mathematically we have

$$I_{incident\_light\_on\_bruise} = I_{incident\_light\_on\_normal\_skin} \tag{3}$$

$$I_{pixel\_intensity\_at\_bruise} = \alpha I_{light\_intensity\_reflected\_from\_normal\_skin} \tag{4}$$

$$I_{pixel\_intensity\_at\_normal\_skin} = \alpha I_{light\_intensity\_reflected\_from\_normal\_skin} \tag{5}$$

where α is a common multiplier for both normal and bruised skin region, reflecting the transfer factor from optical light to image pixel intensity. At this analysis stage, images which contain many pixels of maximum value 255 were discarded due to the possibility of saturation caused by over exposure or by specular reflection, i.e., a non constant α .

Then normalized bruise reflectance (NBR) can be used to eliminate the effects of the unknown incidence light density.

$$NBR = \frac{I_{pixel\_intensity\_at\_bruise}}{I_{pixel\_intensity\_at\_normal\_skin}} \tag{6}$$

The NBR can be regarded as the optical reflectance coefficient of bruise over the optical reflectance coefficient of normal skin. It reflects the contrast shown in a multi-spectral image between bruises and normal skin. At each incidence light wavelength, a NBR value is calculated as the mean intensity of two bruise regions over the mean intensity of 4 random chosen normal skin regions. For one set of bruise images, the NBR value consists of a vector of 12 elements, each element corresponding to a filter passing band center wavelength. In order of acquired image, the NBR vector components are filtered with center wavelengths 1) 370 nm, 2) 415 nm, 3) 460 nm, 4) 480 nm, 5) 540 nm, 6) 555 nm, 7) 560 nm, 8) 577 nm, 9) 650 nm, 10) 800 nm, 11) 970 nm, and 12) no filter.

3. RESULTS

The mean NBR of all bruises in three different age categories were calculated and plotted in Figure 5a against the center wavelength of the filters. The reflectivity dip between 540-577nm indicates high contrast between the bruise and normal skin around these wavelengths. This corresponds to the absorption peak for hemoglobin (see Figure 3). To investigate the bruise age dependence of NBR, the observations were grouped into three age groups. Mean NBR for three bruise age groups <10 days, 10-20 days and >20 days were plotted against the wavelength in Figures 5b, c & d respectively. All NBR curves have a common valley between 540 nm and 577nm regardless of bruise age. This hemoglobin dip is a familiar feature in bruise reflectance curves. It's presence for all age groups reflects the lingering presence of hemoglobin as the dominant chromophore in bruises throughout resolution. The curves have the anticipated trend that the younger bruises appear darker (lower NBRs) and the bruises fade over time, as the overall level of the NBR curves approach one as time progresses. The most noticeable feature of the plots in Figure 5 is the large variance in the data indicated by the error bars on the data points. The error bars represent one standard deviation in either direction. This large variation bodes poorly for discovering a rule for ageing bruises based solely on the ratio of the reflectance of bruised skin over normal skin.

The population for this study, while low on darkly pigmented subjects, should be fairly indicative of the types of variations to be found in an extended care facility. Many of the patients were in poor health, some taking prescribed, blood-altering drugs. Health is one factor that affects healing, and is one variable that leads to high scatter in progress of bruise resolution. Based on the results from this population, we can be certain that no single NBR value can be used

to derive bruise aging information with any acceptable degree of accuracy. We must hope, then, to find other indicators in the data or use additional data to help guide the ageing process.

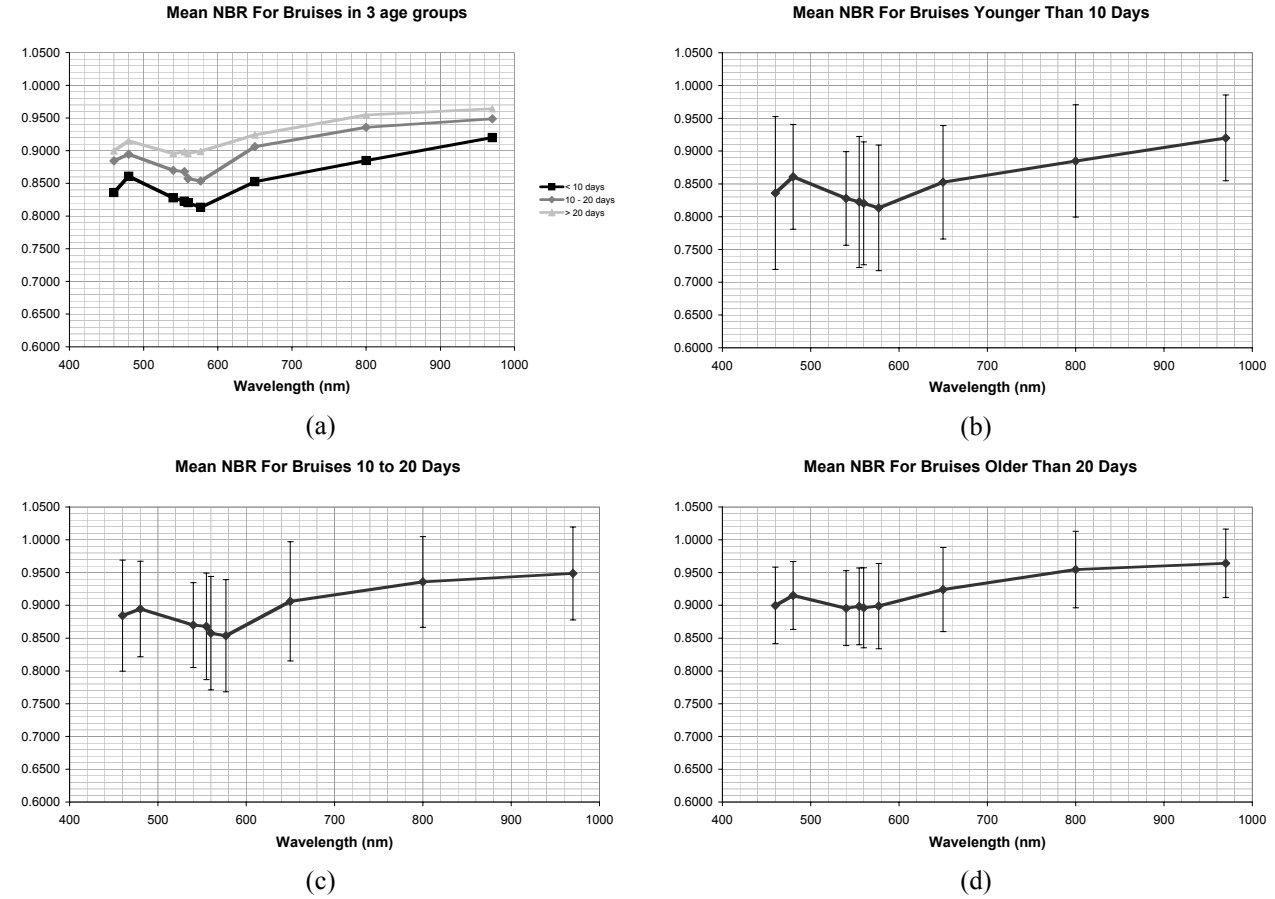

Figure 5. Mean NBR vs wavelength at different bruises ages. (a) the NBR vs wavelength for all bruises included in the study, separated by age groups. (b) NBR for bruises ≤ 10 days old showing std deviation as error bars (c) NBR for bruises aged between 11 and 20 days. (d) NBR for bruises ≥ 21 days old.

Bilirubin has peak absorption at 460nm, which is the first point in the plots. We did not include the data for 370 nm and 415 nm because the signal to noise was very low in the data due to the combination of the low source level from our lights and the low sensitivity of the detector at these wavelengths. Note that the NBR at 460nm is also low. Randerberg, et al. (2004) observed that bilirubin concentration is higher in mid-aged bruises noting that the bilirubin concentration peaked after the hemoglobin concentration for the bruises in their study. In general, the ratio of the absorptions for the bilirubin peak at 460 nm and the absorption within the hemoglobin band from 530 nm to 580 nm is an indicator of the relative concentrations of the bilirubin and hemoglobin chromophores. We represent the absorption by the relationship a = 1 - r, where the total the reflectance and absorbance is one. We look for trends in the value of the absorption in the hemoglobin band relative to the absorption in the bilirubin band by calculating 1-NBR for the two targeted absorption bands. The results for all data are shown in Figure 6.

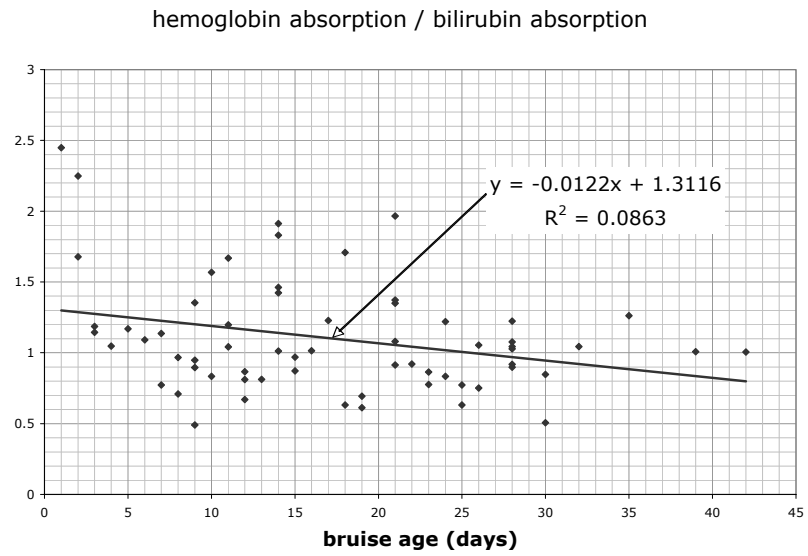

Figure. 6. The ratio of hemoglobin absorption to bilirubin absorption is characterized by (1-NBRhemo)/(1-NBRbili), where the bilirubin absorption is calculated from the the NBR at 460 and the hemoglobin absorption is characterized by mean{(1-NBR540),(1-NBR555),(1-NBR560),(1-NBR570)}.

5. BREAKTHROUGH POINTS.

This is the first report of multi spectral images of bruises acquired in a clinical environment using a realistic population of elder subjects. This study is also one among very few clinical studies of bruise aging based on multi-spectral images. A relatively simple, yet consistent, metric for bruise aging features in multi-spectral images was proposed, but it is concluded that the time histories of NBR will not yield a simple single-point estimation of bruise age with significant certainty. This work has not submitted for publication or presentation elsewhere.

6. CONCLUSION

(1) Bruises show a strong contrast against normal skin at wavelengths centered between 540nm and 577nm, corresponding to the hemoglobin response. This contrast remains as bruises age, as it appears that hemoglobin remains the dominant chromophore throughout the resolution of the bruise..

(2) A simple metric based on the ratio of hemoglobin absorption to bilirubin absorption shows a general trend over time, but a larger data set with some population controls is required to fully understand the response.

(3) Bruises in elderly people show a wide variation of spectral response over time and a wide timeframe to resolution. Some bruises in the study did not resolve after 45 days.

7. REFERENCES

1. National Research Council Panel to Review Risk and Prevalence of Elder Abuse and Neglect. Elder mistreatment: abuse, neglect and exploitaton in an aging America. Washington, D.C.; 2003.
2. National Center on Elder Abuse. National elder abuse incidence study. Washington, D.C.: American Public Human Services Association; 1998.
3. U.S. Department of Health and Human Services AoC, Youth and Families,. Child Maltreatment 2003. Washington DC: U.S. Government Printing Office; 2005.
4. U.S. Department of Health and Human Services - National Center on Child Abuse and Neglect. Third National Incidence Study on Child Abuse and Neglect: Final Report (NIS-3): Washington, D.C.: Government Printing Office; 1996.
5. Wilson EF. Estimation of the age of cutaneous contusions in child abuse. Pediatrics. 1977;60(5):750-2.
6. Langlois NE, Gresham GA. The ageing of bruises: a review and study of the color changes with time. Forensic Sci Int. 1991;50:227-38.
7. Stephenson T. Ageing of bruising in children. J R Soc Med. 1997 Jun 1997;90(6):312-4.

8. Bariciak ED, Plint AC, Gaboury I, Bennett S. Dating of Bruises in Children: An Assessment of Physician Accuracy. Pediatrics. 2003 October 1, 2003;112(4):804-7.
9. Choi, S., et al., *Bruises Literature Review*. 2002, Children and Family Research Center, School of Social Work, University of Illinois at Urbana-Champaign: Urbana, Illinois. p. 17.
10. Maguire, S., et al., *Can you age bruises accurately in children? A systematic review.* Arch Dis Child, 2005. **90**(2): p. 187-189.
11. Schwartz, A.J. and L.R. Ricci, *How accurately can bruises be aged in abused children? Literature review and synthesis.* Pediatrics, 1996. **97**(2): p. 254-257.
12. Stamatas GN, Zmudzka BZ, Kollias N, Beer JZ. Non-invasive measurements of skin pigmentation in situ. Pigment Cell Res. 2004 Dec;17(6):618-26.
13. Randeberg, L.L., et al. Hyperspectral imaging of bruised skin. in Proc. SPIE Vol. 6078: Photonic Therapeutics and Diagnostics II. 2006.
14. Randeberg, L.L., et al. Optical classification of bruises. in Proceedings of SPIE 5312. 2004.